

# Numerical study of Nanofluid flow with heat generation/absorption and Chemical reaction on boundary layer flow over a stretching surface.

Adamu Abdulkadir Tata<sup>\*</sup>, A.G. Madaki<sup>+</sup>, D. G. Yakubu<sup>†</sup>

<sup>\*</sup>Department of Mathematics and Statistics, Federal Polytechnic Bauchi, Bauchi State, Nigeria,

<sup>+</sup>Department of Mathematical Sciences, Abubakar Tafawa Balewa University, P.M.B. 0248, Bauchi, Nigeria.

<sup>†</sup>Department of Mathematical Sciences, Abubakar Tafawa Balewa University, P.M.B. 0248, Bauchi, Nigeria.

---

## Abstract:

This research is mainly concerned with the investigation of the influences of Heat generation/absorption and Chemical reaction over boundary layer flow induced in a nanofluid with two dimensional point along a linearly stretching sheet is studied numerically. The transport equations include the effects of Brownian motion, thermophoresis parameter and other physical parameters are considered. The governing system of partial differential equation is changed into an ordinary differential equation by the use of boundary layer approximation alongside the similarity transformation which is then solved numerically by fourth-fifth order Runge-Kutta Fehlberg method with the shooting technique. The present study uses a convective heating boundary condition. The solutions for the temperature and nanoparticle concentration distributions depend on seven parameters, Heat generation/absorption  $\lambda$ , Chemical reaction  $\gamma$ , Pr, Le, Nb, Nt, Bi are the Prandtl number, Lewis number, the Brownian motion parameter, the thermophoresis parameter, and convection Biot number respectively. The Numerical results on the influence of some physical parameters on temperature as well as nanoparticle concentration profiles are depicted on tables and graphs. The thermal boundary layer thickens with a growth in the indigenous temperature as the Brownian motion, thermophoresis, and convective heating each strengthen. The result of Lewis number on the temperature distribution is negligible. With the other parameters fixed, the local concentration of nanoparticles increases as the convection Biot number increases then decreases as well as the Lewis number increases. For fixed Prandtl number (Pr), Lewis number (Le), and Biot number (Bi), the reduced Nusselt number decreases then the reduced Sherwood number increases as the Brownian motion, thermophoresis and Heat generation/absorption belongings develop stronger.

**Keywords:** Nanofluids, Boundary layer flow, Chemical reaction, stretched surface, Heat generation/absorption, Convective boundary condition

---

Date of Submission: 02-03-2023

Date of acceptance: 13-03-2023

---

## I. INTRODUCTION

Concept of flow of fluid on a stretchable sheet is vigorous in presentations such as hot rolling, extrusion, metal spinning, wire drawing and the rest of them Altan et al. [1], Fisher [2], Tidmore and Klein [3]. That one stands necessary to comprehend the heat and flow features of the progression hence that the completed invention sees the favourite feature terms. The variety of solutions commerce by heat and fluid flow above an extending sheet proceeds remained considered by mutually non-Newtonian and Newtonian fluids and through the presence of carry out magnetic and electric fields, changed thermal boundary conditions, and power law distinction of the stretching velocity. Both comparison as well as direct numerical solutions of the convective transport equations have been stated. A descriptive sample of the current literature on the topic is delivered by references Crane [4], Grupka and Bobba [5], Gupta and Gupta [6], Andersson [7], Dutta et al. [8], Fang [9], Magyaki and Keller [10], Labropulu et al. [11], Prasad et al. [12]. In the previous uncommon years, convective heat transfer in nanofluids has developed a topic of major recent interest. The word "nanofluid" invented by Choi [13] turns a liquid suspension holding ultra-fine particles (diameter less than 50 nm). Investigational studies for example of Masuda et al. [14], Das [15], Pak and Cho [16], Xuan and Li [17], Eastman [18], Minsta [19] indication that level with small nanoparticles concentration (regularly less than 5%), the thermal conductivity of the base liquid is enriched by 10-50% with a significant advance in the convective heat transfer amount. The work on nanofluids has been studied by the following researchers such as Trisaksri and Wongwises [20], Wang and Mujumdar [21], Eastman et al. [22] and also Kakac and Pramuanjaroenkij [23], between some others. These considerations discuss in aspect the work done on convective transport in nanofluids. In a contemporary paper, Boungiorno [24] estimated the different theories explaining the heightened

heat transfer features of nanofluids. He showed that the high heat transfer coefficients in nanofluids cannot be clarified satisfactorily by thermal dispersion phenomenon or increase in turbulence greatness promoted by the manifestation of nanoparticles or nanoparticle revolution as recommended in the literature. He established a logical model for convective transport in nanofluids which receipts into justification the Brownian diffusion and thermophoresis. The Boungiorno [24] model has in recent times been recycled by Kuznetsov and Nield [25] to reading the natural convective flow of a nanofluid over a vertical plate. Recently studies concerning the natural phenomenon of nanofluids, have been investigated by Madaki et al. [27]. The impacts of various dimensionless parameters flow are investigated. Circumventing nanoparticles were initially defined by Choi [13], because their interaction increased thermophysical properties. Temperature distribution in the convection medium for nanofluids was addressed by Buongiorno [24]. Their similarity analysis identified four parameters governing the transport process, namely a Lewis number  $Le$ , a buoyancy-ratio number  $Nr$ , a Brownian motion number  $Nb$ , and a thermophoresis number  $Nt$ . The same authors later extended the work to a nanofluid saturated porous medium Nield and Kuznetsov [26]. In a new paper Khan and Pop [28] previously owned the model of Kuznetsov and Nield [25] to revision the boundary layer flow of a nanofluid past a stretching sheet with a constant surface temperature. Subsequent the work of Khan and Pop [28], it seemed suitable to us to simplify their investigation to a convective boundary condition as a substitute of an isothermal condition. Aziz [29] has earlier used a convective boundary condition to learning the Blasius flow over a flat plate. After his paper, numerous authors have used the convective boundary condition to reconsider the problems that were earlier studied with the isothermal or the isoflux boundary conditions. A limited example are the papers by the following authors: Bataller [30], Yao et al. [31], Makinde and Aziz [32], Makinde and Olanrewaju [33], Magyari [34], Bachok et al. [35], Bachok et al. [36], Ahmad and Pop [37], Yacob et al. [38] and Ishak [39]. In this article paper, our leading detached is to study the influence of a convective boundary condition on boundary layer flow, heat transfer and nanoparticle concentration over a stretching surface in a nanofluid. Moreover, the numerical investigation of nanofluid movement through a squeezed model alongside heat generation/absorption was reported in Madaki et al. [41]. The main boundary layer equations have been converted to a two-point boundary value problem in resemblance variables, and these have been solved numerically. The special effects of embedded physical parameters on fluid velocity, temperature and particle concentration have been presented in graphs. It is expected that the outcomes obtained will not only arrange for useful information for presentations, but also assist as an accompaniment to the previous readings.

In this research, we consider the paper of Makinde and Aziz [40] which the paper name is boundary layer flow of a nanofluid past a stretching sheet with a convective boundary condition. From that we converted partial differential equation into an ordinary differential equation and solved numerically using the fourth-fifth order Runge-Kutta method with the shooting method or technique. Before that, we applying boundary layer approximation to governing equations which we add heat generation/absorption on temperature equation and chemical reaction on concentration equation. The numerical results are presented both in tables and graphs to showing the effects of these physical parameters on thermal and concentration boundary layers.

## II. Mathematical analysis

Deliberate fixed plane  $(x, y)$  boundary layer flow of a nanofluid past a stretching sheet with a linear velocity difference with the distance  $x$  i.e.  $u_w = ax$  where  $a$  is a genuine positive number and  $x$  is the coordinate measured from the position wherever the sheet velocity is zero as shown in Fig. 1 below:

The sheet surface temperature  $T_w$ , to be resolute well ahead, is the result of a convective heating process which is considered by a temperature  $T_f$  and a heat transfer coefficient  $h$ . The nanoparticle concentration  $C$  at the wall is  $C_w$ , though at great values of  $y$ , the significance is  $C_\infty$ . The Boungiorno [24] model may be improved for this problematic to give the following continuousness, momentum, energy, and concentration equations Makinde and Aziz [40]

$$\frac{\partial u}{\partial x} + \frac{\partial v}{\partial y} = 0 \tag{1}$$

$$u \frac{\partial u}{\partial x} + v \frac{\partial u}{\partial y} = -\frac{1}{\rho_f} \frac{\partial p}{\partial x} + \nu \left( \frac{\partial^2 u}{\partial x^2} + \frac{\partial^2 u}{\partial y^2} \right) \tag{2}$$

$$u \frac{\partial v}{\partial x} + v \frac{\partial v}{\partial y} = -\frac{1}{\rho_f} \frac{\partial p}{\partial y} + \nu \left( \frac{\partial^2 v}{\partial x^2} + \frac{\partial^2 v}{\partial y^2} \right) \tag{3}$$

$$\begin{aligned}
 u \frac{\partial T}{\partial x} + v \frac{\partial T}{\partial y} &= \alpha \left( \frac{\partial^2 T}{\partial x^2} + \frac{\partial^2 T}{\partial y^2} \right) + \\
 \tau \left\{ D_B \left( \frac{\partial C}{\partial x} \frac{\partial T}{\partial x} + \frac{\partial C}{\partial y} \frac{\partial T}{\partial y} \right) + \frac{D_T}{T_\infty} \left[ \left( \frac{\partial T}{\partial x} \right)^2 + \left( \frac{\partial T}{\partial y} \right)^2 \right] \right\} \\
 + \frac{Q(x)}{\rho C_p} (T - T_\infty). \tag{4}
 \end{aligned}$$

$$\begin{aligned}
 u \frac{\partial C}{\partial x} + v \frac{\partial C}{\partial y} &= D_B \left( \frac{\partial^2 C}{\partial x^2} + \frac{\partial^2 C}{\partial y^2} \right) + \left( \frac{D_T}{T_\infty} \right) \left( \frac{\partial^2 T}{\partial x^2} + \frac{\partial^2 T}{\partial y^2} \right) \\
 - K_1 (C - C_\infty). \tag{5}
 \end{aligned}$$

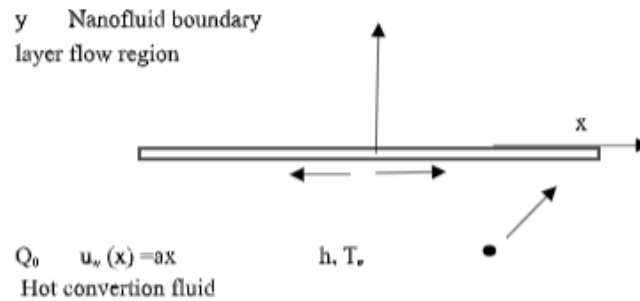


Figure 1. geometry of the problem

where  $u$  is the velocity component along the  $x$  direction and  $v$  is the velocity component along the  $y$  direction, and also  $p$  is the fluid pressure,  $\rho_f$  is the density of base fluid,  $\nu$  is the kinematic viscosity of the base fluid,  $\alpha$  is the thermal diffusivity of the base fluid,  $\tau = (\rho c)_p / (\rho c)_f$  is the ratio of nanoparticle heat capacity and the base fluid heat capacity,  $D_B$  is the Brownian diffusion coefficient,  $D_T$  is the thermophoretic diffusion coefficient and lastly  $T$  is the local temperature. The subscript  $\infty$  indicates the principles at big values of  $y$  wherever the fluid is gentle. The boundary conditions may be written as follows:

$$y = 0, u = ax, v = 0, -k \frac{\partial T}{\partial y} = h(T_f - T), C = C_\infty \tag{6}$$

$$y \rightarrow \infty, u = 0, v = 0, T = T_\infty, C = C_\infty \tag{7}$$

With dimensionless quantities

$$\eta = (a/\nu)^{1/2} y, \psi = (a\nu)^{1/2} x f(\eta), \theta = \frac{T - T_\infty}{T_f - T_\infty} \Rightarrow T = \theta T_f,$$

$$\phi = \frac{C - C_\infty}{C_w - C_\infty} \Rightarrow C = \phi C_w \tag{8}$$

Anywhere  $\psi$  is the stream function with  $u = \partial\psi/\partial y, v = -\partial\psi/\partial x$ .

Therefore, using an order level enquiry of the  $y$ -direction momentum equation (normal to the street) using a boundary layer approximation above.

$v \ll u$

$$\frac{\partial u}{\partial x}, \frac{\partial v}{\partial x}, \frac{\partial v}{\partial y}, \frac{\partial^2 u}{\partial x^2} \ll \frac{\partial u}{\partial y} \text{ and } \frac{\partial^2 u}{\partial y^2}.$$

$$\frac{\partial p}{\partial y} = 0.$$

Therefore, neglecting the pressure slope in the y path, the momentum, temperature, and concentration equations and the boundary conditions reduce to the following system of correspondence equations.

$$f''' + ff'' - f'^2 = 0 \quad (9).$$

$$\theta' + Pr f\theta' + Pr Nb\phi'\theta' + Pr Nt\theta'^2 + Pr \lambda(\theta) = 0 \quad (10).$$

$$\phi'' + Le f\phi' + \frac{Nt}{Nb}\theta'' - \gamma\phi = 0 \quad (11).$$

With the following boundary conditions;

$$f(0) = 0, f'(0) = 1, \theta' = -Bi(1 - \theta(0)), \phi(0) = 1 \quad (12).$$

$$f'(\infty) = 0, \theta(\infty) = 0, \phi(\infty) = 0 \quad (13).$$

wherever primes signify differentiation with detail to  $\eta$  and the seven parameters seeming in Equations. (9-12) are defined as follows,

$$Pr = \frac{\nu}{D_B}, Nb = \frac{\tau D_B C_w}{\nu}, Nt = \frac{\tau D_T T_f}{T_\infty \nu}, Le = \frac{\nu}{D_B}, \tau = \frac{(\rho C_p)}{(\rho C_f)},$$

$$\frac{Nt}{Nb} = \frac{D_T T_F}{D_B C_w T_\infty}, \gamma = \frac{K_1 \nu (C_w - C_\infty)}{a D_B C_w}, Bi = \frac{h(\nu/a)^{1/2}}{k}.$$

$$\lambda = \frac{Q(x)}{a T_f} (T_f - T_\infty) \quad (14).$$

Through  $Nb = 0$ , there is no thermal transportation due to buoyancy special effects formed as an outcome of nanoparticle concentration slopes. Here, we remind that Equation (9) together with the resultant boundary conditions on  $f$  providing by Equation (12) has a sealed form solution which is known by

$$f(\eta) = 1 - e^{-\eta} \quad (15).$$

From Equation (14), where  $Pr, Nt, Nb, Le, \gamma, Bi$  and  $\lambda$ , represent Prandtl number, thermophoresis, Brownian motion parameter, Lewis number, Chemical reaction parameter, Biot number and heat generation/absorption, respectively. The reduced Nusselt number  $Nur$  and the reduced Sherwood number  $Shr$  may create in terms of the dimensionless temperature at the sheet surface,  $\theta'(0)$  and the dimensionless concentration at the sheet surface,  $\phi'(0)$ , respectively i.e.

$$Nur = Re_x^{-1/2} Nu = -\theta'(0) \quad (16),$$

$$Shr = Re_x^{-1/2} Sh = -\phi'(0) \quad (17),$$

where

$$Nu = \frac{q_w x}{k(T_w - T_\infty)}, Sh = \frac{q_m x}{D_B(\phi_w - \phi_\infty)}, Re_x = \frac{u_w(x)x}{\nu} \quad (18).$$

where  $q_w$  is the surface (wall) heat flux and  $q_m$  is the surface (wall) mass flux.

Table 1

Comparison of effects for the reduced Nusselt number ( $-\theta'(0)$ ) and reduced Sherwood number ( $-\phi'(0)$ ) with

$Le=10, Pr=10, Bi=\infty, \lambda=\gamma=0.$

Makinde and Aziz [40] Present results					
Nb.	Nt.	Nur.	Shr.	Nur. (present)	Shr. (present)
0.10	0.10	0.9524	2.1294	0.9355	2.1262
0.20	0.10	0.5056	2.3819	0.4927	2.3839

0.30	0.10	0.2522	2.4100	0.2490	2.4240
0.40	0.10	0.1194	2.3997	0.1188	2.4002
0.50	0.10	0.0543	2.3836	0.0541	2.3824
0.10	0.20	0.6932	2.2740	0.6780	2.2754
0.10	0.30	0.5201	2.5286	0.5203	2.5218
0.10	0.40	0.4026	2.7952	0.3994	2.7960
0.10	0.50	0.3211	3.0351	0.3216	3.0352

Table 2

Computation of the reduced Nusselt number Nur. ( $-\theta'(0)$ ) and reduced Sherwood number Shr. ( $-\phi'(0)$ ) with  $Le=10, Pr=10, Bi=\infty$ .

Nb.	Nt.	$\lambda$	$\gamma$	Nur. (present)	Shr. (present)
0.10	0.10	0.1	0.1	0.7405	2.4238
0.10	0.10	0.2	0.2	0.5265	2.5831
0.10	0.10	0.3	0.3	0.2871	2.7580
0.10	0.10	0.4	0.4	0.0114	2.9548
0.10	0.10	-0.1	0.1	1.1156	2.1378
0.10	0.10	-0.2	0.2	1.2839	2.0069
0.10	0.10	-0.3	0.3	1.4423	1.8822
0.10	0.10	-0.4	0.4	1.5924	1.7629

III. Results and discussion

In this part, the varying procedure of the relevant parameters, numerical results for the Nusselt number, the Sherwood number, temperature, and nanoparticle concentration profiles were constructed and immensely discussed. Figures (2-18) shows the data collected for the temperature profile, Nusselt number profile, the Sherwood number profile as well as the nanoparticle concentration profile, Madaki et al [41]. Its accuracy and strength have been repeatedly confirmed in our previous publication Makinde and Aziz [40]. As a further check on the accuracy of our numerical computations as follows in Tables.

Table 3

Computation show the reduced Nusselt number Nur. ( $-\theta'(0)$ ) while  $Le=10.0, Pr=10.0, Bi=0.10, \lambda=\gamma=0$ .

Nt.	Nur. (Nb=0.1)	Nur. (Nb=0.2)	Nur. (Nb=0.3)	Nur. (Nb=0.4)	Nur. (Nb=0.5)
0.1	0.0928	0.0871	0.0763	0.0587	0.0372
0.2	0.0926	0.0865	0.0744	0.0542	0.0313
0.3	0.0924	0.0858	0.0721	0.0489	0.0258
0.4	0.0922	0.0850	0.0693	0.0430	0.0209
0.5	0.0920	0.0841	0.0657	0.0370	0.0171

Table 4

Computation show the reduced Sherwood number Shr. ( $-\phi'(0)$ ) when  $Pr=10.0, Le=10.0, Bi=0.10, \lambda=\gamma=0$ .

Nt.	Shr. (Nb=0.1)	Shr. (Nb=0.2)	Shr. (Nb=0.3)	Shr. (Nb=0.4)	Shr. (Nb=0.5)
0.10	2.3861	2.4192	2.4385	2.4547	2.4646
0.20	2.3607	2.4279	2.4687	2.5025	2.5183
0.30	2.3379	2.4402	2.5055	2.5568	2.5707
0.40	2.3177	2.4568	2.5501	2.6153	2.6180
0.50	2.3006	2.4784	2.6038	2.6734	2.6581

Table 5

Comparison showing the reduced Nusselt number Nur. ( $-\theta'(0)$ ), reduced Sherwood number Shr. ( $-\phi'(0)$ ) and surface temperature ( $-\theta(0)$ ) with  $Nt=0.5, Nb=0.5, \lambda=0, \gamma=0$ .

Makinde and Aziz [40] present results								
Pr.	Bi.	Le.	Nur.	Shr.	$\theta(0)$	Nur.	Shr.	$\theta(0)$
1	0.1	5	0.0789	1.5477	0.2107	0.0801	1.5434	0.2100

2	0.1	5	0.0806	1.5554	0.1988	0.0806	1.5585	0.1970
5	0.1	5	0.0735	1.5983	0.2655	0.0719	1.5957	0.2650
10	0.1	5	0.0387	1.7293	0.6132	0.0387	1.7266	0.6132
5	1.0	5	0.1476	1.6914	0.8524	0.1456	1.6985	0.8540
5	10.0	5	0.1550	1.7122	0.9845	0.1599	1.7121	0.9800
5	100.0	5	0.1557	1.7144	0.9984	0.1556	1.7145	0.9900
5	$\infty$	5	0.1557	1.7146	1.0000	0.1556	1.7146	1.0000
5	0.1	10	0.0647	2.3920	0.3531	0.0639	2.4007	0.3540
5	0.1	15	0.0600	2.9899	0.4001	0.0594	2.9894	0.4002
5	0.1	20	0.0570	3.4881	0.4296	0.0566	3.4887	0.4287

Table 1 contains a comparison of our results for the reduced Nusselt number and the reduced Sherwood number with those reported by Makinde and Aziz [40] for  $Le = 10$ ,  $Pr = 10$ ,  $Bi = \infty$ . The infinitely large Biot number simulates the isothermal stretching model used in Makinde and Aziz [40] as well-known earlier. The consequences for all arrangement values of Brownian motion parameter ( $Nb$ ) and thermophoresis parameter ( $Nt$ ) used in our computations, showed close to among our results and the results reported in Makinde and Aziz [40]. From the first five entries illustration that for a secure thermophoresis parameter,  $Nt = 0.1$ , the reduced Nusselt number decreases suddenly with the intensification in Brownian motion, that as Brownian motion ( $Nb$ ) is improved from 0.1 to 0.5. Conversely, the reduced Sherwood number rises substantially as  $Nb$  is increased from 0.1 to 0.2 but inclines to plateau beyond  $Nb = 0.2$ . As well as the Brownian motion strengthens, it influences a larger amount of the fluid, affecting the thermal boundary layer to condense, which in go declines the reduced Nusselt number. The thickening of the boundary layer due to tougher Brownian motion will be emphasized again when the temperature profiles are conversed. It determination be seen from the Concentration profiles seeming later in the Conversation that the initial slope of the curve and the level of the concentration boundary layer are not affected significantly beyond  $Nb = 0.2$  and hence the plateau in the Sherwood number performance. From the last four entries in Table 1 indication that the reduced Nusselt number decreases as the thermophoresis diffusion enters bottomless into the fluid and sources the thermal boundary layer to set. But, the increase in the thermophoresis parameter ( $Nt$ ) improves the Sherwood number, a decision that is reliable with the results of Makinde and Aziz [40].

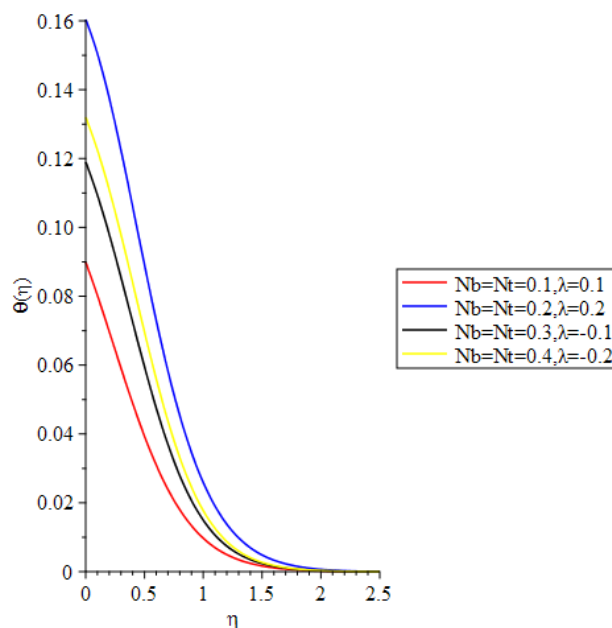
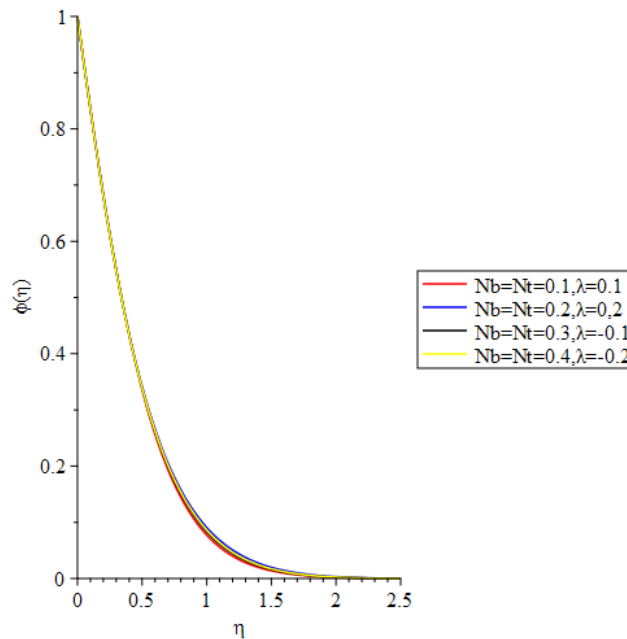


Figure 2: effects of Brownian motion, thermophoresis and heat generation / absorption on temperature profile when  $Bi=0.1$ ,  $Le=5$ ,  $Pr=5$ ,  $\gamma = 0.1$ .



**Figure 3:effects of Brownian motion, thermophoresis and heat generation / absorption on nanoparticles concentration profile when  $Bi=0.1$ ,  $Le=5$ ,  $Pr=5$ ,  $\gamma=0.1$ .**

Table 2, show the computation of reduced Nusselt number and reduced Sherwood number when  $Le=10$ ,  $Pr=10$  and  $Bi=\infty$ , the reduced Nusselt number is increases when  $\lambda>0$  and decreases when  $\lambda<0$  while reduced Sherwood number is decreases when  $\lambda>0$  as well as  $\lambda<0$  is increases.

Table 3 arrange for a trial of our outcomes for the reduced Nusselt number when the stretching sheet is heated convectively. The Biot number of 0.1 denotes a weak convective heating condition. Since, the current work is the second attempt on expecting the thermal flow in a nanofluid due to a linearly stretching sheet, a relativevaluation of the outcomes in Table 3 with the other published outcomes is not possible. Nevertheless, the superb agreement between our outcomes and those of others for the restrictivecircumstances as seen in Tables 1 and 3 provides us assurance in the greatcorrectness of the results delivered in Table 3. The outcomes in Table 3 show that when the Brownian motion is weak ( $Nb = 0.1$ ), the transformation in the strength of thermophoretic influence has little effect on the reduced Nusselt number and hence the heat transfer procedure. But, when the Brownian motion is relatively strong ( $Nb = 0.5$ ), the thermophoretic consequenceuses a strong effect on the heat transfer; decreasing it by almost 50% as thermophoresis parameter variations from 0.1 to 0.5. This show it is exactly with the results of Makinde and Aziz [40].The reduced Sherwood number data matching to the data of Table 3 is obtainable in Table 4. Excluding for  $Nb = 0.1$ , the reduced Sherwood number rises by a little percent as the thermophoretic effect strengthens. The extremeintensification of round 8% is perceived to befall at  $Nb = 0.5$ .This showing a similar with the results of Makinde and Aziz [40].

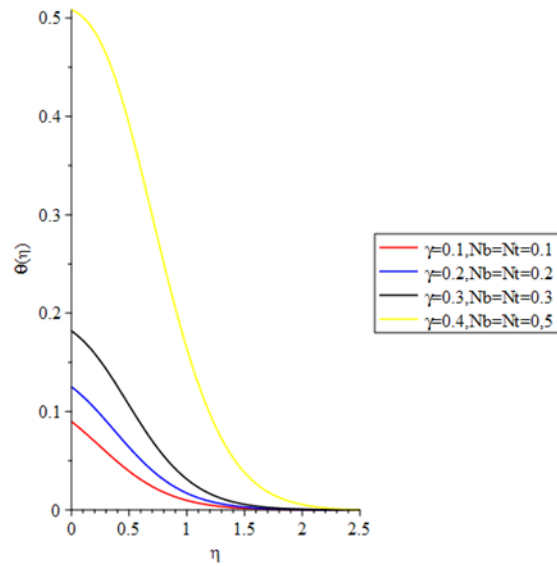


Figure 4: effect of Brownian motion, thermophoresis and chemical reaction on temperature profile when  $Bi=0.1, Le=5, Pr=5, \gamma=0.1$

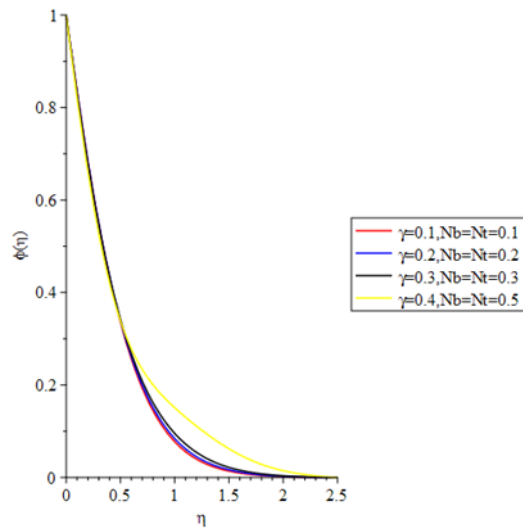
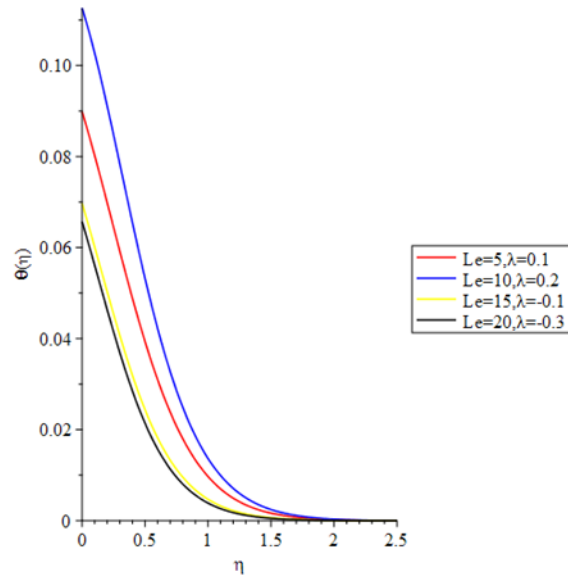
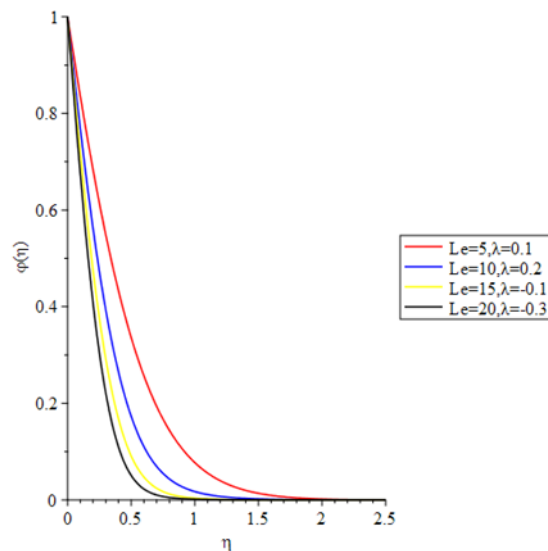


Figure 5: result of Brownian motion, thermophoresis and Chemical reaction on nanoparticle concentration profile with  $Bi=0.1, Le=5, Pr=5, \gamma=0.1$





**Figure 6: effects of Lewis number and heat generation / absorption on temperature profile when Nb= 0.1, Nt=0.1, Bi=0.1, Pr=5.  $\gamma=0.1$ .**



**Figure 7: effects of Lewis number and heat generation / absorption on nanoparticles concentration profile when Nt= 0.1, Nb= 0.1, Bi=0.1, Pr=5.  $\gamma=0.1$ .**

Table 5, showing the special effects of Lewis number, Prandtl number and Biot number on the reduced Sherwood numbers and reduced Nusselt number then the surface temperature of the stretching sheet. The thermophoresis and the Brownian motion parameters remained permanent at 0.5 each. From the first four entries illustration that the alteration in Prandtl number from 1.0 to 2.0 has only trivial effect on reduced Nusselt number, reduced Sherwood number and surface temperature ( $\theta(0)$ ), but then as the Prandtl number (Pr) rises further, there is a significant reduction in reduced Nusselt number ( $N_{ur}$ ) and a significant rise in reduced Sherwood number ( $Sh_r$ ) and surface temperature ( $\theta(0)$ ). The next four entries in the Table 5 gives that for Pr =5, Le =5, the rise in Bi from 1.0 to 10.0 rises the reduced Nusselt number and the surface temperature, but then the adjustment in reduced Sherwood number is quite slight. Therefore, a more tenfold growth in Bi from 10 to 100 has only small consequence on the reduced Nusselt number, the reduced Sherwood number, and the surface temperature. The result of Lewis number can be seen by inspecting the last three entries in the Table 5. When the followings Pr and Bi stable at 5.0 and 0.1, separately, an intensification in Lewis number reasons the reduced Nusselt number to decline but then rise the reduced Sherwood number and the surface temperature.

Therefore, as a results, there was a fascinating agreement between the current and past investigations. We now turn our attention to the conversation of graphical consequences that provide additional understandings into the problem under analysis.

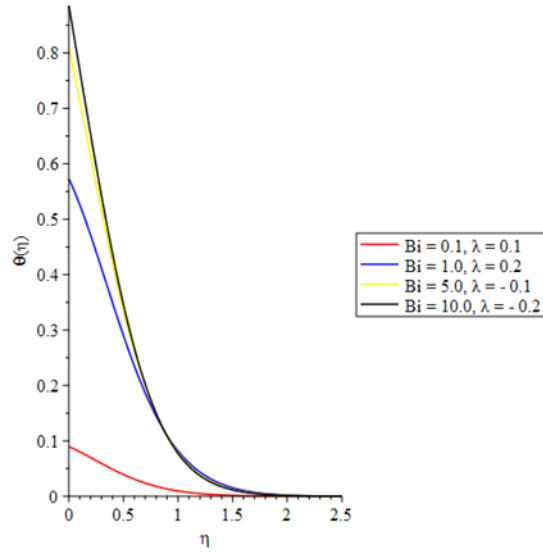


Figure 8: effects of Bi and heat generation/absorption on temperature profile when  $Nt=0.1$ ,  $Nb=0.1$ ,  $Le=Pr=5$ ,  $\gamma=0.1$ .

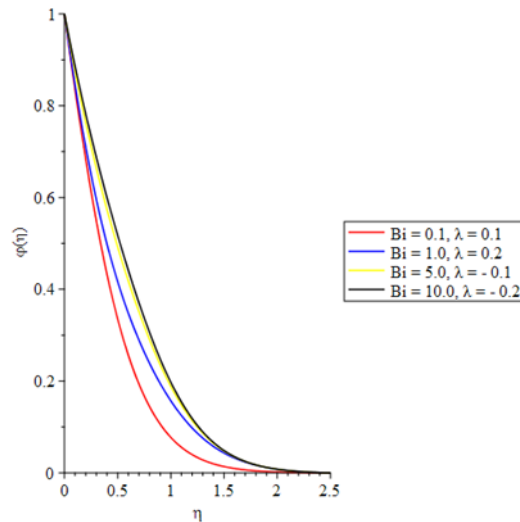


Figure 9: effects of Bi and heat generation/absorption on nanoparticle concentration profile when  $Nt=0.1$ ,  $Nb=0.1$ ,  $Le=5$ ,  $Pr=5$ ,  $\gamma=0.1$ .

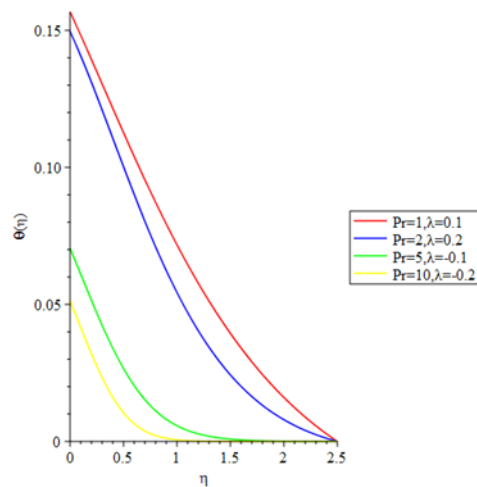


Figure 10: effects of Prandtl number and Heat generation/absorption on temperature profile with  $Nt=0.1$ ,  $Nb=0.1$ ,  $Bi=0.1$ ,  $Le=5$ ,  $\gamma=0.1$ .

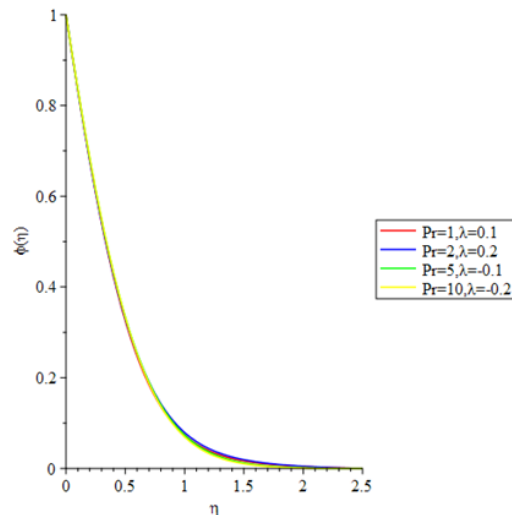


Figure 11: effects of Prandtl number and Heat generation/absorption on nanoparticle concentration profile with  $Nt=0.1$ ,  $Nb=0.1$ ,  $Bi=0.1$ ,  $Le=5$ ,  $\gamma=0.1$ .

## 1. Graphical results

### Temperature profiles

Figure 2 indicates the temperature distributions in the thermal boundary layer for altered values of the Brownian motion, the thermophoresis parameters and heat generation/absorption. As both  $Nb$ ,  $Nt$  and  $\lambda > 0$  or  $\lambda < 0$  intensification, the boundary layer stiffens, as prominent earlier in deliberating the tabular data, the surface temperature growths, and the curves become less sharp indicating a decrease of the reduced Nusselt number. As realised in Figure 4, the outcome of Brownian motion, thermophoresis parameter and Chemical reaction parameter on temperature profile as  $Nb$ ,  $Nt$  and Chemical reaction parameter increase and surface temperature would increase. The figure 6 would show the result of Lewis number on the temperature profiles is obvious only in a region near to the sheet as the curves tend to unite at larger distances from the sheet with the  $\lambda < 0$  and  $\lambda > 0$  as Lewis number and heat generation/absorption increase then surface temperature increase. However, the figure 16 illustrates result of Lewis number and Chemical reaction parameter as increase the surface temperature would increase and the thickness of the boundary layer grows significantly as  $Le$  increases. Figure 8 illustrates the effect of Biot number and heat generation/absorption on the thermal boundary layer. As likely, the robust convection effects in greater surface temperatures, affecting the thermal result to penetrate yawning into the inactive fluid. The figure 14 gives effect of Biot number and Chemical reaction which both increases then surface temperature increase. The temperature profiles showed in Figure 10 appearance that as the Prandtl number rises with heat generation/absorption, the depth of the thermal boundary layer drops as the curves become gradually vertical. The temperature profile of figure 18 show, the effect of Prandtl number and Chemical reaction as increases, the thickness of the thermal boundary layer decreases. The effect of Heat generation/absorption on temperature profile is show in figure 12 when  $\lambda$  is increase, the temperature would increase. For a result, the reduced Nusselt number, being proportionate to the initial gradient, rises. This form is significant of the free convective boundary layer flow in a consistent fluid, Incropera and Dewitt [42].

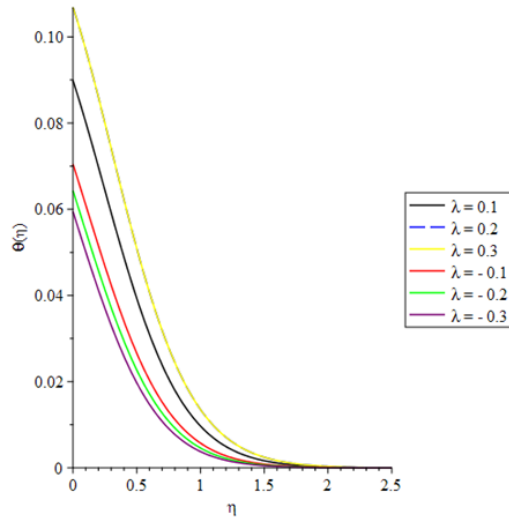


Figure 12: effect of  $\lambda > 0$  and  $\lambda < 0$  on temperature profile with  $Le = 5, Pr = 5, Nt = 0.1, Nb = 0.1, \gamma=0.1$  and  $Bi = 0.1$ .

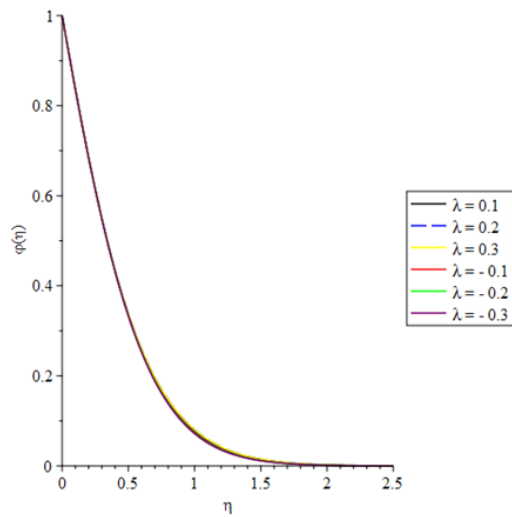


Figure 13: effects of heat generation / absorption on nanoparticle concentration profile with  $Le = 5, Pr = 5, Nt = 0.1, Nb = 0.1, \gamma=0.1$  and  $Bi = 0.1$ .

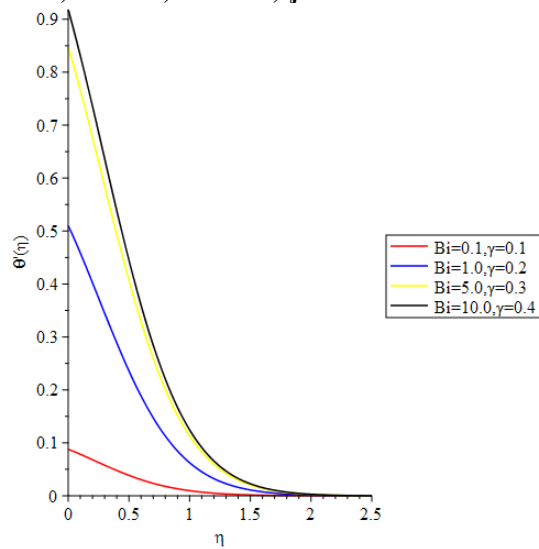


Figure 14: effect of  $Bi$  and Chemical reaction on temperature profile with  $Le= 5, Pr=5, Nb=0.1, Nt=0.1, \lambda=0.1$ .

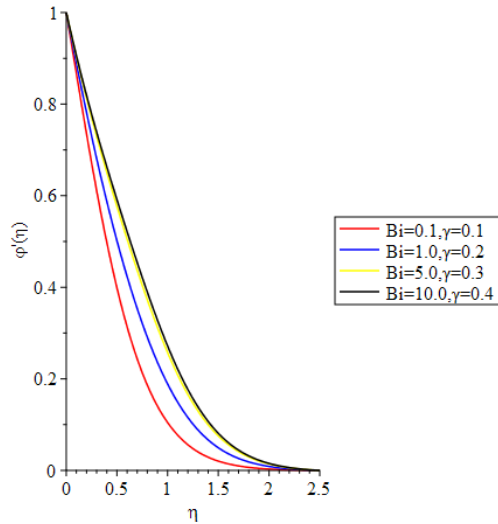


Figure 15: effect of Bi and Chemical reaction parameter on nanoparticle concentration with  $Le=Pr=5$ ,  $Nb=Nt=0.1$ ,  $\lambda=0.1$

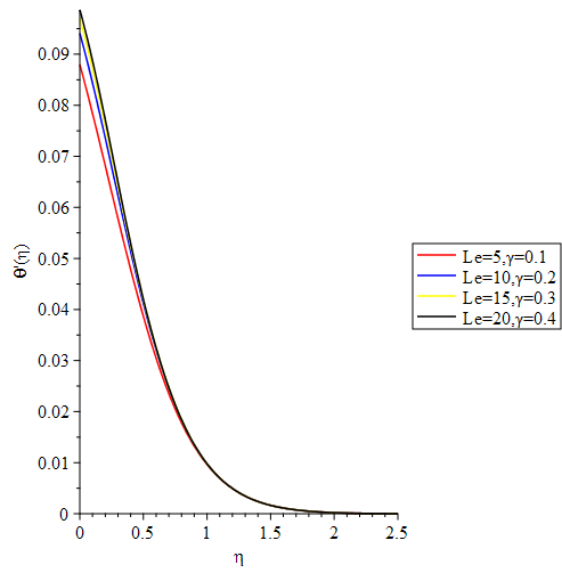
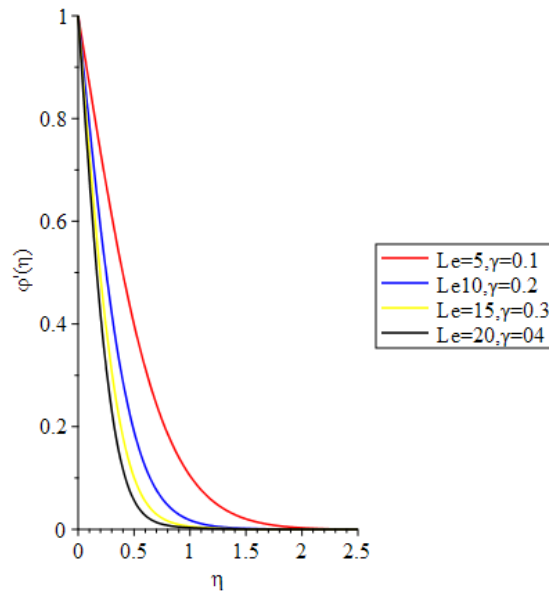


Figure 16: effect of Lewis number and Chemical reaction on temperature profile with  $Nb=0.1$ ,  $Nt=0.1$ ,  $Pr=5$ ,  $Bi=0.1$ ,  $\lambda=0.1$ .



**Figure 17: effect of Lewis number and Chemical reaction on concentration profile when  $Nb=0.1, Nt=0.1, Pr=5, Bi=0.1, \lambda=0.1$ .**

### Concentration profiles

The nanoparticle concentration consistent to Figure 2 is presented in Figure 3. Distinct temperature profiles, concentration profiles are only faintly affected by the force of the Brownian motion, thermophoresis and Heat generation/absorption. The figure 5 show the effects of Brownian motion, thermophoresis and Chemical reaction on concentration profiles which slightly affected them. The figure 5 is corresponding to figure 4. An appraisal of Figure 6 and Figure 7 expressions that the Lewis number and Heat generation/absorption meaningfully disturbs the concentration distribution (Figure 7), but then has slight effect on the temperature distribution (Figure 3). Used for a base fluid of definite

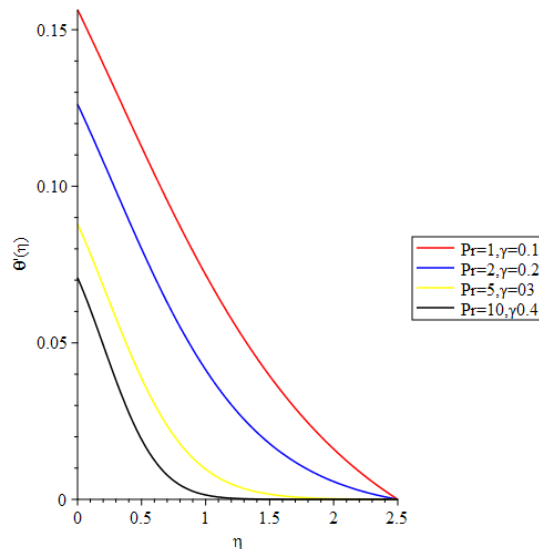


**Figure 18: effect of prandtl number and Chemical reaction on temperature profiles with  $Nb=Nt=Bi=\lambda=0.1, Le=5$ .**

kinematic viscosity  $\nu$ , a developed Lewis denotes a lower Brownian diffusion coefficient  $D_B$  (see Equation(14)) which must consequence in a smaller penetration deepness for the concentration boundary layer. This is an accurately what we perceive in Figure 7. Similar with the figures 16 and 17 the effects Lewis number and Chemical reaction on temperature and nanoparticle concentration profiles. It was observed in Figure 8 that as the convective heating of the slip is boosted i.e.  $Bi$  intensifications, the thermal penetration deepness rises. Because the concentration distribution is determined through the temperature field, one expects that a greater Biot number would stimulate a wide penetration of the concentration. This expectation is indeed realized in

Figure 9 which expects higher concentrations at greater ideals of the Biot number. Figure 15 show effect of Lewis number and Chemical reaction with higher concentrations at the higher values of the Biot number. Lastly, the figure 13 gave effect of Chemical reaction on nanoparticle concentration.

#### IV. Conclusions

The numerical learning of the heat generation/absorption and chemical reaction going on boundary layer flow in a nanofluid encouraged as a consequence of the motion of a linearly stretching sheet has existed implemented. The procedure of a convective heating boundary condition in its place of a constant temperature or a constant heat flux creates this study more general innovative. The succeeding conclusions are consequent.

1. The transportation of momentum, temperature, and nanoparticles concentration in the relevant boundary layers be governed by on seven physical parameters: Heat generation/absorption  $\lambda$ , Brownian motion parameter  $N_b$ , thermophoresis parameter  $N_t$ , Prandtl number  $Pr$ , Lewis number  $Le$ , Chemical reaction parameter  $\gamma$  and convection Biot number  $Bi$ .
2. For extremely large Biot number describing the convective heating (which matches to the relentless temperature boundary condition), the contemporary results and those stated by Makinde and Aziz [40] equal up to four places of decimal.
3. For stable Prandtl number  $Pr$ , Lewis number  $Le$ , and convective Biot number  $Bi$ , the current boundary condenses and the local temperature increases as the Brownian motion, thermophoresis special effects increase in level. A comparable effect on the thermal boundary is perceived when Brownian motion ( $N_b$ ), thermophoresis ( $N_t$ ), Lewis number ( $Le$ ), and Biot number ( $Bi$ ) are reserved fixed and the is Prandtl number ( $Pr$ ) enlarged or when Prandtl number ( $Pr$ ), Brownian motion ( $N_b$ ), thermophoresis ( $N_t$ ), and Lewis number ( $Le$ ) are kept fixed and the Biot number is improved. Conversely, when Prandtl number ( $Pr$ ), thermophoresis ( $N_t$ ), Brownian motion ( $N_b$ ), and Biot number ( $Bi$ ) are kept stable, and the Lewis number is enlarged, the temperature distribution is exaggerated only insignificantly.
4. Through the intensification in Biot number, the concentration layer sets but the concentration layer becomes higher as Lewis number rises.
5. For permanent Prandtl number ( $Pr$ ), Lewis number ( $Le$ ), and Biot number ( $Bi$ ), the reduced Nusselt number declines but the reduced Sherwood number rises as the Brownian motion and thermophoresis effects rise in level.

#### REFERENCES

- [1]. Altan T., Oh S., Gegel H. (1979). Metal Forming Fundamentals and Applications. American Society of Metals, Metals Park, OH.
- [2]. E.G. Fisher. (1976). Extrusion of Plastics. Wiley, New York.
- [3]. Tidmore Z., Klein I. (1970). Engineering Principles of Plasticating Extrusion, Polymer Science and Engineering Series. Van Norstrand, New York.
- [4]. Crane I.J. (1970). Flow past a stretching plane, J. Appl. Math. Phys. (ZAMP) 21, 645-647.
- [5]. Grupka J.L., Bobba K.M. (1985). Heat transfer characteristics of a continuous stretching surface with variable temperature, J. Heat Transfer 107, 248-250.
- [6]. Gupta P.S., Gupta A.S. (1977). Heat and mass transfer on a stretching sheet with suction or blowing, Can. J. Chem. Eng. 55, 744-746.
- [7]. Andersson H.I. (2002). Slip flow past a stretching surface, Acta Mech. 158, 121-125.
- [8]. Dutta B.K., Roy P., Gupta A.S. (1985). Temperature field in flow over a stretching sheet with uniform heat flux, Int. Commun. Heat Mass Transfer 12, 89-94.
- [9]. Fang T. (2008). Flow and heat transfer characteristics of boundary layers over a stretching surface with a uniform-shear free stream, Int. J. Heat Mass Transf. 51, 2199-2213.
- [10]. Magyari E., Keller B. (2000). Exact solutions of boundary layer equations for a stretching wall, Eur. J. Mech. B-Fluids 19, 109-122.
- [11]. Labropulu F., Li D., Pop I. (2010) Non-orthogonal stagnation-point flow towards a stretching surface in a non-Newtonian fluid with heat transfer, Int. J. Therm. Sci. 49, 1042-1050.
- [12]. Prasad K.V., Vajravelu K., Dutt P.S. (2010). The effects of variable fluid properties on the hydro-magnetic flow and heat transfer over a non-linearly stretching sheet, Int. J. Therm. Sci. 40, 603-610.
- [13]. Choi S.U.S. (1995). Enhancing thermal conductivity of fluids with nanoparticles, in: Developments and Applications of Non-Newtonian Flows, FED-vol. 231/MD vol. 66, pp. 99-105.
- [14]. Masuda H., Ebata A., Teramea K., Hishinuma N. (1993). Altering the thermal conductivity and viscosity of liquid by dispersing ultra-fine particles, Netsu Bussei 4 (4), 227-233.
- [15]. Das S. (2003) Temperature dependence of thermal conductivity enhancement for nanofluids, J. Heat Transfer 125, 567-574.
- [16]. Pak B.C., Cho Y. (1998). Hydrodynamic and heat transfer study of dispersed fluids with submicron metallic oxide particles, Exp. Heat Transfer 11, 151-170.

- [17]. Xuan Y., Li Q. (2003). Investigation on convective heat transfer and flow features of nanofluids, *J. Heat Transfer* 125, 151-155.
- [18]. Eastman J.A., Choi S.U.S., Li S., Yu W., Thompson L.J. (2001). Anomalous increased effective thermal conductivity of ethylene glycol-based nanofluids containing copper nanoparticles, *Appl. Phys. Lett.* 78 (6), 718-720.
- [19]. Minsta H.A., Roy G., Nguyen C.T., Doucet D. (2009). New temperature dependent thermal conductivity data for water-based nanofluids, *Int. J. Therm. Sci.* 48, 363-371.
- [20]. Trisaksri V., Wongwises S. (2007) Critical review of heat transfer characteristics of nanofluids, *Renew. Sust. Energ. Rev.* 11, 512-523.
- [21]. Wang X.-Q., Mujumdar A.S. (2007). Heat transfer characteristics of nanofluids: a review, *Int. J. Therm. Sci.* 46, 1-19.
- [22]. Eastman J.A., Phillpot S.R., Choi S.U.S., Keblinski P. (2004). Thermal transport in nanofluids, *Annu. Rev. Mater. Res.* 34, 219-246.
- [23]. Kakac S., Pramaumjaroenkij A. (2009). Review of convective heat transfer enhancement with nanofluids, *Int. J. Heat Mass Transf.* 52, 3187-3196.
- [24]. Buongiorno J. (2006). Convective transport in nanofluids, *J. Heat Transfer* 128, 240-250.
- [25]. Kuznetsov A.V., Nield D.A. (2010). Natural convective boundary-layer flow of a nanofluid past a vertical plate, *Int. J. Therm. Sci.* 49, 243-247.
- [26]. Nield D.A., Kuznetsov A.V. (2009). The Cheng-Minkowycz problem for natural convective boundary-layer flow in a porous medium saturated by a nanofluid, *Int. J. Heat Mass Transf.* 52, 5792-5795.
- [27]. Madaki A.G., Hussaini A.A., Kabiru S.A., Barde A., Adamu A.T. (2022). Numerical study on the influence of thermophoresis and magnetic field on boundary layer flow over a moving surface in a nanofluid, *IJSRMT* 2, 4- 9.
- [28]. Khan W.A., Pop I. (2010). Boundary-layer flow of a nanofluid past a stretching sheet, *Int. J. Heat Mass Transf.* 53, 2477-2483.
- [29]. Aziz A. (2009). A similarity solution for laminar thermal boundary over a flat plate with a convective boundary condition, *Commun. Nonlinear Sci. Numer. Simulat.* 14, 1064-1068.
- [30]. Bataller R.C. (2008). Similarity solutions for flow and heat transfer of a quiescent fluid over a nonlinearly stretching surface, *J. Mater. Process Technol.* 203, 176-183.
- [31]. Yao S., Fang T., Zhong Y. (2011). Heat transfer of a generalized stretching/shrinking wall problem with convective boundary conditions, *Commun. Nonlinear Sci. Numer. Simulat.* 16, 752-760.
- [32]. Makinde O.D., Aziz A. (2010). MHD mixed convection from a vertical plate embedded in a porous medium with a convective boundary condition, *Int. J. Therm. Sci.* 49 (2010) 1813-1820.
- [33]. Makinde O.D., Olanrewaju P.O. (2010). Buoyancy effects on thermal boundary layer over a vertical plate with a convective surface boundary condition, *Trans. ASME e J. Fluids Eng.* 132, 044502(1-4).
- [34]. Magyari E. (2011). Comment on "A similarity solution for laminar thermal boundary layer over a flat plate with a convective surface boundary condition" by A. Aziz, *Comm. Nonlinear Sci. Numer. Simul.* 2009;14:1064-8, *Commun. Nonlinear Sci. Numer. Simulat.* 16, 599-601.
- [35]. Bachok N., Ishak A., Pop I. (2010). Boundary-layer flow of nanofluids over a moving surface in a flowing fluid, *Int. J. Therm. Sci.* 49, 1663- 1668.
- [36]. Bachok N., Ishak A., Nazar R., Pop I. (2010). Flow and heat transfer at a general three-dimensional stagnation point in a nanofluid, *Physica B* 405, 4914-4918.
- [37]. Ahmad S., Pop I. (2010). Mixed convection boundary layer flow from a vertical flat plate embedded in a porous medium filled with nanofluids, *Int. Commun. Heat Mass Transfer* 37, 987-991.
- [38]. Yacob N.A., Ishak A., Pop I. (2011). Falkner-Skan problem for a static or moving wedge in nanofluids, *Int. J. Therm. Sci.* 50, 133-139.
- [39]. Ishak A. (2010). Similarity solutions for flow and heat transfer over a permeable surface with convective boundary conditions, *Appl. Math. Comput.* 217, 837-842.
- [40]. Makinde O.D and Aziz A. (2011), Boundary layer flow of a nanofluid past a stretching sheet with a with convective boundary condition. *Int. J. Therm. Sci.* 50, 1326-1332.
- [41]. Madaki A.G., Roslan R., Rusiman M.S., Raju C.S.K. (2018). Analytical and numerical solutions of squeezing unsteady Cu and TiO<sub>2</sub>-nanofluid flow in the presence of thermal radiation and heat generation/absorption. *Alexandria Engineering Journal*, (2018) 57, 1033-1040.
- [42]. Incropera F.P., Dewit D.P. (1996). Introduction to Heat Transfer, third ed. Wiley, New York, p. 453.